CoA NOTE MAT. No. 24

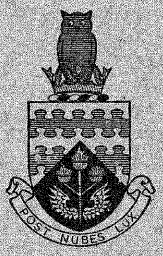

THE COLLEGE OF AERONAUTICS
CRANFIELD

SOME FURTHER EXPERIMENTS IN FATIGUE TESTING AT 20 kHz

by

B. S. Hockenhull

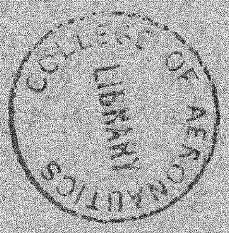

CoA Note Mat. No. 24

October, 1968

THE COLLEGE OF AERONAUTICS

DEPARTMENT OF MATERIALS

Some further experiments in fatigue testing at 20 kHz

- by -

B.S. Hockenhull

SUMMARY

Considerations are made of the suitability of acoustic transformers applied to fatigue testing at 20 kHz. A suitable system has been constructed which allows the use of plain cylindrical specimens. The results of fatigue tests on an aluminium alloy are given and discussed in relation to structure and environment.

Contents

Introduction

A number of papers have appeared recently (1,2,3,4,5,6,7) indicating an interest in fatigue tests conducted at high frequencies (10^4 Hz). This is principally associated with two factors, (a) the accelerated evaluation of fatigue properties and (b) the effect of frequency on fatigue properties together with data collection at particular frequencies.

Some papers (4,5,6) have given details of techniques for high frequency testing, mainly based on electrostrictive and magnetostrictive resonant devices, and results have been obtained indicating frequency effects in a number of materials (1,6,7).

In general, the systems described use specimens of relatively complex shape and this paper describes the development of an existing system to use plain cylindrical specimens together with improved stress level measurement.

Previous work

The system previously described (5) consists basically of a half wave length magnetostrictive transducer to one end of which is attached a resonant, stepped amplitude transformer. The other end is fitted with a crystal transducer for the feedback signal. The specimen, of dumb-bell shape, is attached to the free, high amplitude end of the transformer. A schematic diagram of the system is shown in Fig. 1. The design of the specimens used is based on some stress amplification in the specimen itself, in order to avoid overloading the transducer-transformer system.

Neppiras(4) has discussed specimen shapes of this form, usually symmetrically tapered or dumb-bell shaped with a cylindrical central region. In the latter type, stress concentrations above those calculated from an area ratio arise at the discontinuity unless very careful preparative techniques are adopted. In all these types, an advantage is that the highly stressed volume is kept small so that a marked temperature rise is avoided with high damping materials and satisfactory strain levels can be attained. In the case of symmetrically tapered dumb-bell specimens the nominal peak stress level in the specimen is derived from measurements of the longitudinal displacement amplitude as a function of distance along the specimen. The slope of this curve at the displacement node then gives the maximum strain and from this and a dynamic Young's modulus, the stress level is deduced. The measurements may be made either directly with a travelling microscope or by a photographic technique (7). In either case the process may be inaccurate and too lengthy to complete in the real lifetime of the specimen, particularly at higher stress levels.

Many of these difficulties could in principle be overcome by the use of a plain cylindrical specimen and efforts have been made to accomplish this.

Design considerations

The simplest plain cylindrical specimen is a half wavelength stub of the material to be tested, having displacement antinodes at each end and hence, if the strain distribution is sinusoidal, a peak strain at the central displacement node. Since there is no amplification in the specimen itself, it is clear that the maximum strain in a simple stepped transformer will be at least the same as that in the specimen. In such a case, the material from which the transformer is made is clearly important. It is worthwhile considering this further.

Suppose the wavelength in the transformer and specimen material are λ_1 and λ_2 respectively. Assuming tensile strains only, let $x = 0$ at the displacement node of the transducer, and $x = \lambda_1/4$ at the high amplitude end. Then at any point x_1 in the high amplitude stub the displacement ξ_1 is given by

$$\xi_1 = \xi_{max} \sin(2\pi x_1/\lambda_1)$$

where ξ_{max} is the maximum displacement.

The strain ϵ_1 is given by

$$\epsilon_1 = \frac{d\xi_1}{dx} = \frac{2\pi\xi_{max}}{\lambda_1} \cos(2\pi x_1/\lambda_1).$$

The maximum strain ϵ_{max} occurs at $x_1 = 0$ and is therefore

$$\epsilon_{max} = \frac{2\pi\xi_{max}}{\lambda_1}$$

The maximum stress in the transformer is then

$$\sigma_{1_{max}} = \frac{2\pi E_1 \xi_{max}}{\lambda_1} \qquad (1)$$

where E_1 is the dynamic Young's modulus for the transformer material. If the frequency, fixed by the transducer-transformer system is ν, then $\lambda = \frac{c}{\nu}$ where c is the velocity of the stress wave propagation and

$$\sigma_{1_{max}} = 2\pi \xi_{max} \frac{E_1}{c_1} \qquad \nu = \omega \xi_{max} \frac{E_1}{c_1} \text{ where } \omega = 2\pi\nu,$$

where c_1 refers to the transformer material.

Similarly, for a simple half wavelength cylindrical specimen,

$$\sigma_{2_{max}} = \omega \xi_{max} \frac{E_2}{c_2}$$

where E_2 and c_2 refer to the specimen material.

If the endurance limit stress is $\sigma_\ell/E = \epsilon_\ell$, i.e. $\sigma_\ell = E\epsilon_\ell$. For the specimen to break, $\sigma_{2max} > E_2\epsilon_{\ell_2}$

i.e. $$c_2\epsilon_{\ell_2} < \omega\,\xi_{max} \qquad (2)$$

Similarly, for no failure of the transformer, $c_1\epsilon_{\ell_2} > \omega\,\xi_{max}$

i.e. $$c_1\epsilon_{\ell_1} > c_2\epsilon_{\ell_2} \qquad (3)$$

for failure of the specimen without failure of the transformer. Thus, the quantity $c_1\epsilon_{\ell_1}$ is a measure of the merit of the suitability of material for transformer use. Some typical values of $c\epsilon_\ell$ for a number of materials are given in Table I. It will be seen that titanium alloys are likely to be best although aluminium alloys have faily good values. The other property of interest in the transformer material is the internal friction which should be low at the required frequency. In this respect the aluminium alloys are good, probably followed by titanium alloys.

A further design requirement in the transformer is the magnification ratio M, which is the ratio of the amplitudes at the high and low amplitude ends. This is chosen to give a suitable end amplitude in the specimen to provide the alternating stress levels required. At the same time, it is desirable that the flexural compliance of the system be low in order to minimize the possibility of the generation of transverse modes.

The geometrical factors concerned with the design of high amplitude resonant transformers have been discussed extensively by Eisner[8,9] who derives a non-dimensional parameter Φ called the figure of merit using more general arguments. Examination of the parameter Φ leads to similar conclusions to the above, regarding the materials suitable for transformers.

Eisner[9] has derived transformer shapes and has made comparisons of several types. Figure 2, due to Eisner, indicates three major types. The Fourier type which is based on a fourth-order Fourier cosine series represents a compromise between the required high figure of merit attainable and high flexural compliance associated with the exponential form and the low figure of merit with a low flexural compliance in the case of a simple stepped shape and therefore appears suitable for this work.

Experimental Work

A magnetostrictively driven system was already available and it was decided to construct a two-stage system based on this. The two stages chosen were a simple 10:1 magnification stepped transformer followed by either 5:1 or 10:1 magnification Fourier transformers. This would give end amplitudes of up to 0.2 mm at the end of the system.

The stepped transformer was brass, and aluminium alloys (L65 and RR58) were chosen for the Fourier transformer. Design parameters for these,

depended on an accurate value of the wavelength in the alloys at the resonant frequency of the system being known. This was measured directly by cutting a plain cylindrical sample from the alloy to be used and measuring its resonant frequency when attached to the transducer-stepped transformer system. It was possible to measure the resonant length to within 0.1% and thus to find the wavelength to within 0.01 mm.

A suitable profile was constructed from the data and the transformer was cut on a profiling lathe. The finishing was by hand polishing with 600 grade emery paper. Threaded studs were adopted for attachment both to the stepped transformer and the specimen. The transformer system is shown diagrammatically in Figure 3 and the assembled equipment in Figure 4.

Specimens of several materials were prepared in the form of plain cylindrical rods of length $\lambda/2$ appropriate to the material. The amplitude at the free and fixed ends of the specimen were measured during resonance and it was found that the amplitudes were within 3% of each other in all cases and within 2% for the aluminium alloys. Measurements of the double amplitude were made with a travelling microscope fitted with a micrometer eyepiece and by plotting the amplitude as a function of distance along the specimen, the distribution of amplitude along the specimen was shown to be sinusoidal. The stress level in any specimen is determined for a single amplitude measurement a. Thus, if a is the measured double amplitude, then:

$$\sigma_{max} = \frac{2\pi}{\lambda} E \frac{a}{2} = \frac{\pi E a}{\lambda} = \frac{\pi E a}{2\ell}$$

where ℓ is the specimen length. a is easily measured to within about $\pm 10^{-4}$ cm. giving an accuracy of $\pm$ 1% at the lowest stress levels. The dynamic modulus used to convert the strain level to a stress level was determined for the material by resonance at the test frequency.

Since failure of the specimen is indicated by a fall in amplitude of the crystal output as the crack propagated, the counter system was arranged to cut-off with a fall of about 5% in amplitude. The feedback crystal output was monitored and always showed harmonics at some point immediately before the amplitude started to fall, indicating the presence of a crack. However, this indication is not sufficiently sensitive to say at what point in the life of the specimen the crack was present.

For the aluminium alloys tested the rise in temperature of the specimen was usually only a few degrees centigrade. In these cases therefore, no cooling (which would in any case alter the environmental condition) was used. For a copper specimen tested the rise in temperature during the test was about 70°C.

A number of fatigue tests have been carried out using this system. In most cases, failure of the specimen occurred within 0.5 cm. of the displacement nodal plane in which region the stress level is within about 1% of the maximum value. A few failures occurred well away from the nodal

plane but this was associated with one of two features, either (a) a lack of surface preparation, for example in the case of tests made on an extruded material, or (b) end failures close to the drilled and tapped hole in the specimen.

In the first case, surface preparation by electrolytic polishing was found to give a more consistent behaviour and as in previous experiments[7] this preparation, using Lenoir's solution, was adopted as a standard for all the tests on Aluminium alloys. In the few cases where such specimens failed well away from the nodal plane, failure was associated with a polishing pit. In the second case, the end failures were probably associated with the operation of transverse modes to produce large bending stresses at this point. Careful preparation of the specimen ends to ensure their flatness and adjustment of the phase shift control has alleviated but not prevented this kind of failure.

Fatigue tests have been made principally on an Al-Cu-Mg alloy, RR58, which is an age-hardening alloy of considerable interest in the aeronautical field. Table II gives the composition and heat treatment of the alloy.

Results and Discussion

The apparatus satisfactorily fatigues plain cylindrical specimens of materials where the damping is sufficiently low to prevent any large temperature rises. The end amplitude of the specimens varies only slightly during the tests on some aluminium alloys in the aged condition. In the case of other metals tested, such as copper, the temperature rise and the small amplitudes possible are limiting factors in the fatigue test.

The fatigue results in the form of stress/log cycles to failure curves are given for RR58, both for dumb-bell specimens and the plain cylindrical specimens in Figs. 5 and 6.

The results from the two specimen goemetries are rather different although both show a frequency effect in that S - log N curve is displaced at the higher frequency to a larger number of cycles to failure for a given stress level. The strain level measurements in the dumb-bell specimen case are however relatively crude and the stress level less certain because of the complex shape. These features are considered to account for the observed differences.

When the results of figure 6 are plotted on the basis of real time to failure against frequency as in figure 7 then the effect is clearly seen to vary with stress level. It will be seen that at the lowest stress level the time to failure in the high frequency case exceeds that for the low frequency test. This may have no significance other than that the fatigue limit has been raised at high frequency although it has been observed[10] that the increase in number of cycles to failure is never so large as to give an extension of real time to failure. Wade and Grootenhuis[1] have noted that the time to failure in a series of tests on an aluminium alloy

RR56 are about the same over a range of frequencies from 850 to 3800 Hz. This is apparently a similar effect to that in the present series of tests. It may be concluded therefore that a real frequency effect exists and that for this material the fatigue limit is raised.

The fractures exhibit characteristic fatigue markings. Figure 8 shows a crack in a high frequency fatigued specimen with associated persistent slip markings. There is little in the fracture surface to characterise the high frequency failures which are mainly flat transverse failures with a small shear lip at the initiation point. In the propagation region, a few areas are visible showing ripples associated with Stage II cracking. In such areas, as for example in figure 9 - the spacing is small, averaging 0.3 μm and they are rather irregular in comparison to low frequency ripples noted by Forsyth[11]. However, at this spacing, if the ripples correspond to the stress cycles, then the whole Stage II propagation would occupy only a small fraction of the total life, that is about 1 or 2 secs. in real time. The most notable features of the Stage I regions, i.e. in the shear zones leading from the initiation point, are tear dimples and predominance of cleavage. Further fractographic studies are now being made using scanning electron microscopy and replication techniques.

A few preliminary high frequency tests in the presence of small amounts of water on the specimens show that there is a strong effect, the life decreasing sharply in the presence of water. An extensive programme of environmental testing is currently being undertaken.

At present it appears that the frequency effect in aluminium alloys is associated with inhibition of the initiation stage of the fatigue failure process. It is probable that environment has a strong effect here although recent experiments by Horden[12]suggest that for aluminium there is little change in crack nucleation rate in vacuo as compared to air.

It is likely also that the plastic strain amplitude is lower at higher frequencies and indeed Thompson and Wadsworth have suggested that this will cause a frequency effect at least in the case of materials which are not prone to atmospheric corrosion[13].

So far as fatigue in metallurgically metastable materials is concerned, recent work[14]has discussed evidence that quite small irradiations with ultrasonic energy can produce relatively large changes in diffusivity and this, insofar as it affects the fatigue process will also contribute to the frequency effect.

In the case of the age hardening aluminium alloys therefore it would be expected that the differences in substructure found subsequent to fatigue might vary with frequency. Evidence of this is being sought using thin foil electron microscopy.

It seems likely therefore, that although the high frequency fatigue test is an accelerated test, at least at stress levels significantly above the fatigue limit, the possibility of establishing a simple correlation with

low frequency data is unlikely. However, the evaluation potential of such a test is such that it would be worthwhile to examine the possibility of whether the order of fatigue strength of a material at low and high frequencies is the same. So far there is no evidence that this is not so.

References

1. Wade, A.R. and Grottenhuis, P. — Very high speed fatigue testing. Int. Conf. on Fatigue Metals, Inst. Mech. Engrs. 1956, Paper 5.

2. Neppiras, E.A. — Metal Fatigue at high frequency, Proc. Phys. Soc. Sect. B, Vol. 70, 1957, p. 393.

3. Stephenson, N. — A review of the literature on the effect of frequency on the fatigue properties of metals and alloys. N.G.T.E. M.320, June, 1958.

4. Neppiras, E.A. — Techniques and equipment for fatigue testing at very high frequencies. Proc. ASTM Vol. 59, 1959, p. 691.

5. Clifton, T.E., Hockenhull, B.S., and Sollars, A.R. — The development and evaluation of an ultrasonic fatigue unit. College of Aeronautics Note No. 141, March, 1963.

6. Kikukawa, M., Ohji, K., and Ogura, K. — High frequency push-pull fatigue strength of metal up to 49.7 kc/sec. Proc. of Seventh Japan Congress on testing materials. Soc. of Materials Science, Japan, 1964.

7. Hockenhull, B.S. — Fatigue in some Aluminium Alloys at 20 kc/sec. Physics and Non-destructive testing. Ed. by W.J. McGonnagle, Gordon and Breach, 1967.

8. Eisner, E. — The Design of Sonic amplitude transformers for high magnification. Jnl. Acoust. Soc. of America, Vol. 35, No. 9, 1397, Sept. 1963.

9. Eisner, E., and Seager, J.S. — A longitudinally resonant stub for vibrations of large amplitude. Ultrasonics, April-June, 1965.

10. Kennedy, A.J. — Processes of Creep and Fatigue in Metals. Oliver and Boyd, p. 313.

11. Forsyth, P.J.E. — A two stage process of fatigue crack growth. Proc. Symposium on Crack Propagation. Cranfield, September, 1961.

12. Hordon, M.J. — Fatigue behaviour of aluminium in vacuum. Act. Met. Vol. 14, No. 10, Oct. 1966.

13. Thompson, N., and Wadsworth, N.J. — Advances in Physics 7, 72, 1958.

14. Brown, A.F. — The effect of vibrational deformation on diffusion - controlled reactions in metals. Appl. Materials Research, Vol. 5, No. 2, April, 1966.

TABLE I

Properties of acoustic transformer materials

Material	C ϵ_1 (velocity x limiting fatigue strain) cm/sec.	Internal Friction
Copper	470	High
Mild Steel	600	High
Ti alloy (Hylite 50)	2500	Moderate
Al alloy L65	1180	Low
Al alloy RR58	1260	Low

TABLE II

Hiduminium R.R.58 - Extruded rod form.

Composition Cu 2.5 Mg 1.5 Fe 1.0 Ni 1.2 Ti 0.1 Bal Al.

Density: 2.75 $g.ml^{-1}$

Heat Treatment Solution treatment $2\frac{1}{2}$ hours 530°C
10 sec. air cool - water quench
Aged 10 hours at 190°C.

Typical tensile properties.

Tensile strength 27 tonf in^{-2}

Elongation 12%

TABLE III

Design data for typical Fourier transformer

Calculated from data by Eisner[9]. For material RR58 (See Table II)

λ = 12.3 cm at 20.1 kHz Magnification ratio 5:1

Length (from low amplitude end) (in)	Diameter (in)
0	1.000
1.254	1.000
1.570	0.999
1.725	0.996
1.880	0.992
2.040	0.983
2.195	0.970
2.352	0.951
2.508	0.926
2.665	0.894
2.822	0.855
2.980	0.811
3.135	0.764
3.292	0.716
3.445	0.667
3.606	0.620
3.763	0.575
3.920	0.535
4.076	0.497
4.233	0.464
4.389	0.43[illegible]
4.546	0.410
4.703	0.387
4.860	0.367
5.017	0.351
5.174	0.337
5.330	0.325
5.487	0.315
5.644	0.307
5.800	0.302
5.957	0.298
6.114	0.295

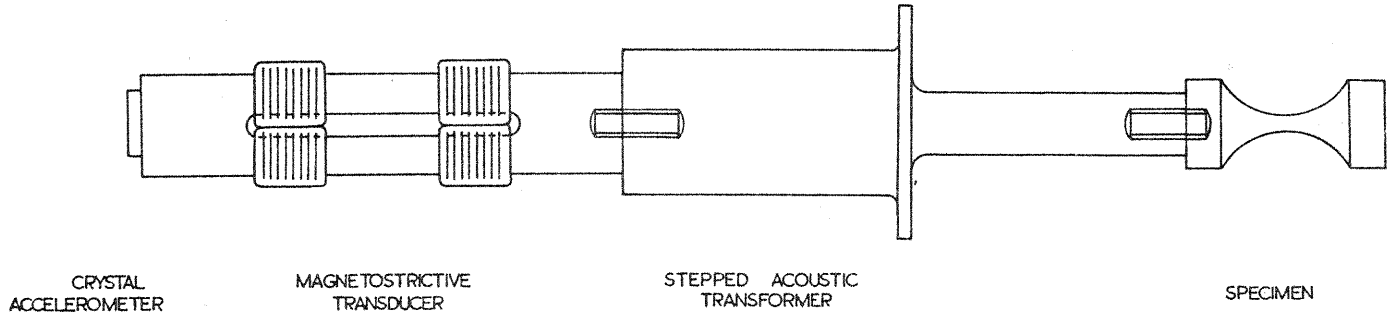

FIG. 1 SCHEMATIC ARRANGEMENT OF ORIGINAL SYSTEM.

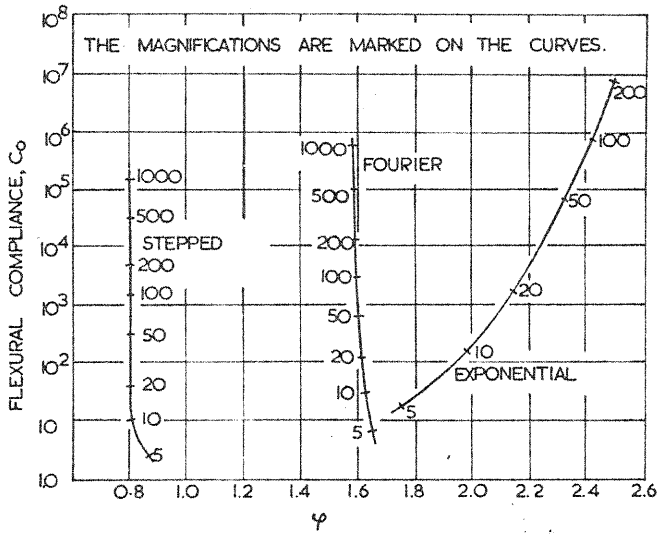

FIG. 2. FLEXURAL COMPLIANCE AND FIGURE OF MERIT FOR THREE TYPES OF TRANSFORMER. AFTER EISNER[8].

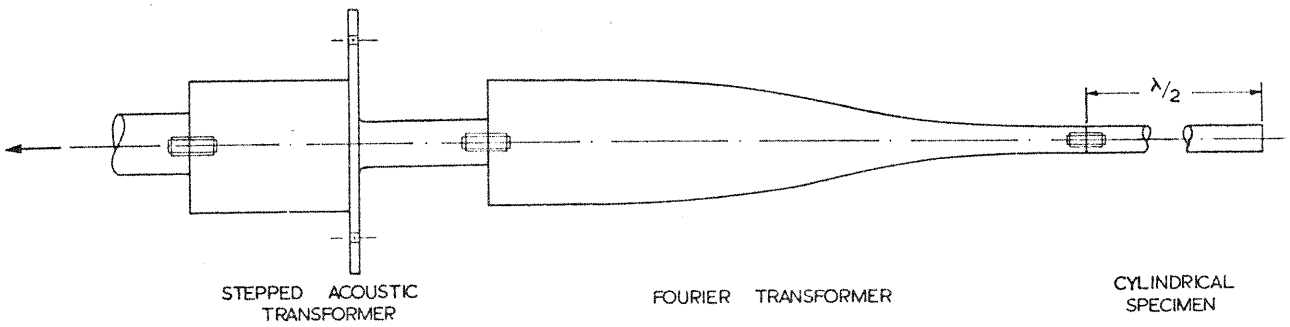

FIG. 3. SCHEMATIC ARRANGEMENT OF LATER SYSTEMS.

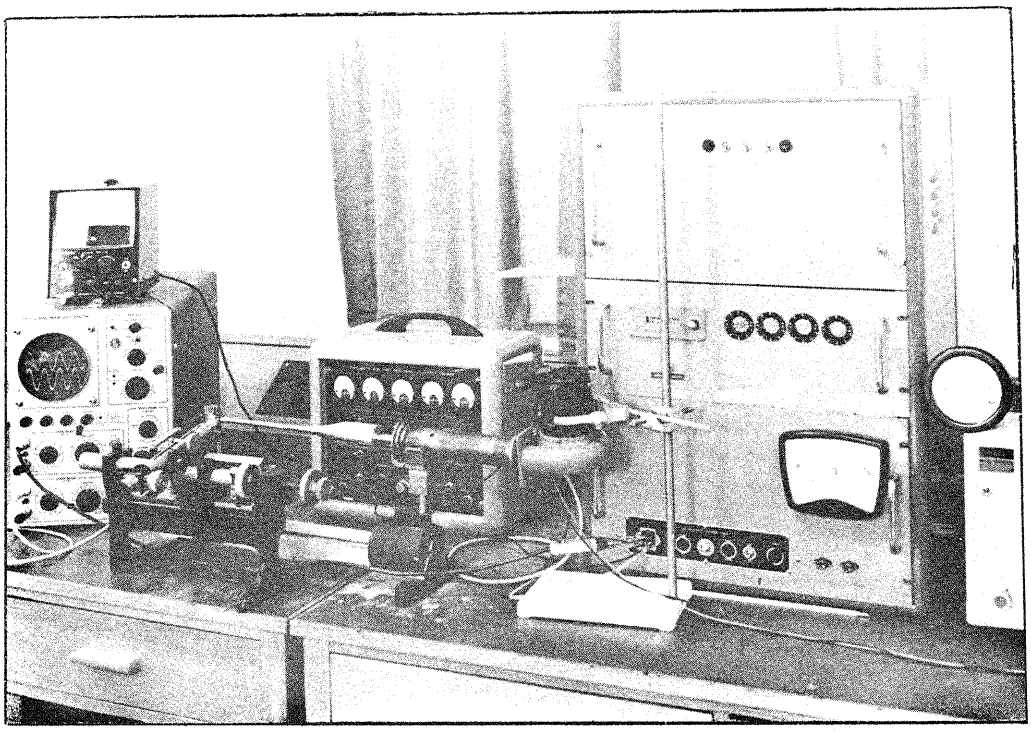

FIG. 4 HIGH FREQUENCY FATIGUE SYSTEM

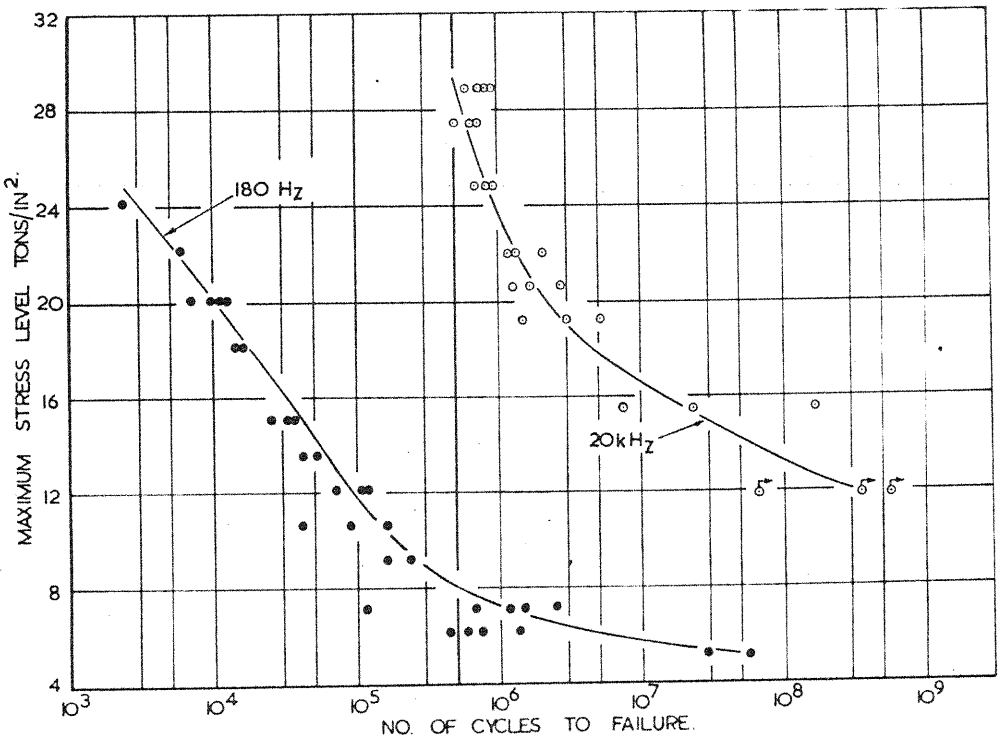

FIG. 5. COMPARATIVE FATIGUE DATA ON RR 58. IN OPTIMUM AGED CONDITION FOR DUMBELL SPECIMENS.

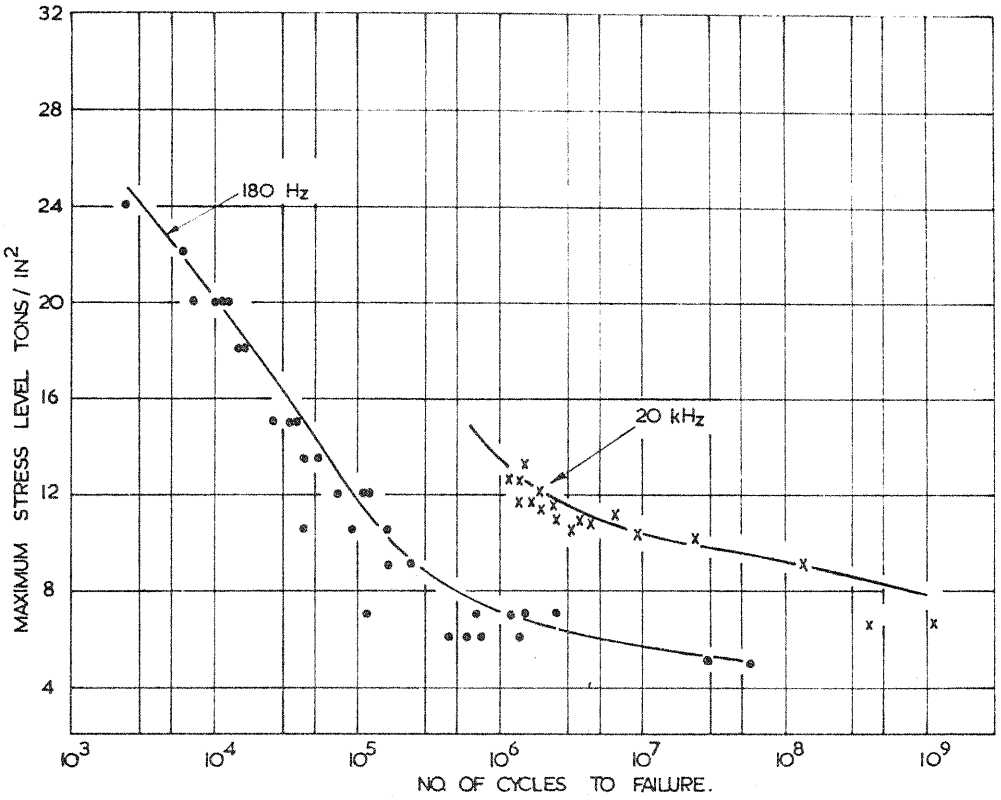

FIG. 6. COMPARATIVE FATIGUE DATA ON RR.58. IN OPTIMUM AGED CONDITION FOR PLAIN CYLINDRICAL SPECIMENS.

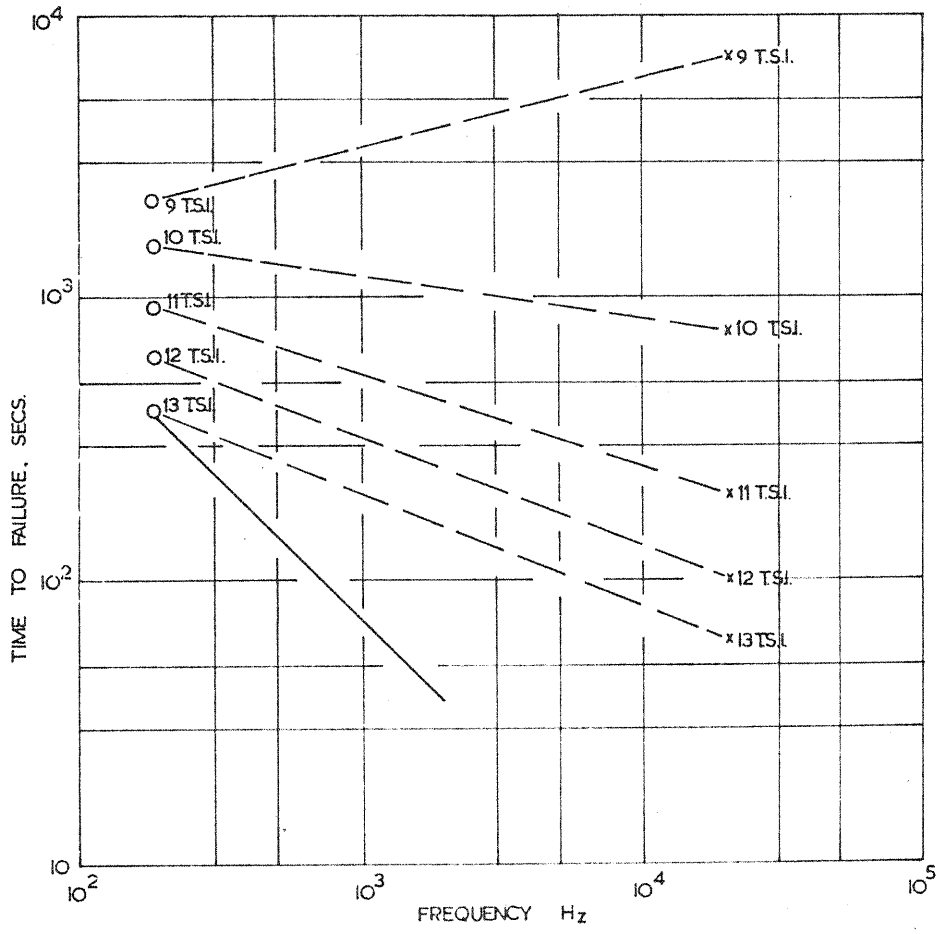

FIG. 7. TIME TO FAILURE FOR TWO FREQUENCIES.

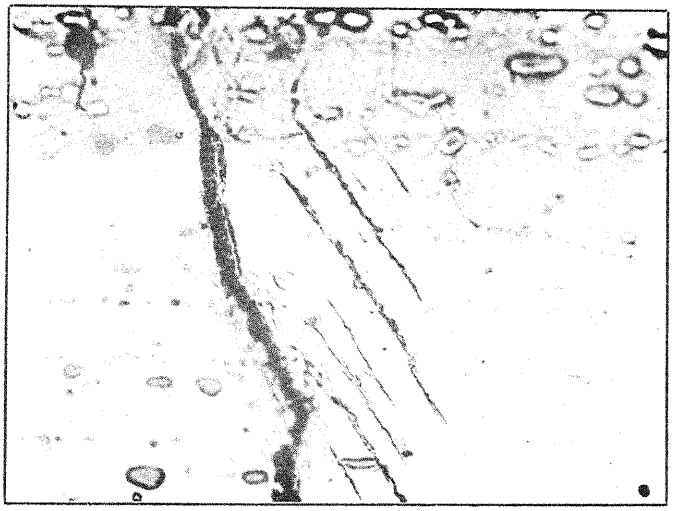

FIG. 8 FATIGUE CRACK PRODUCED AT HIGH FREQUENCY

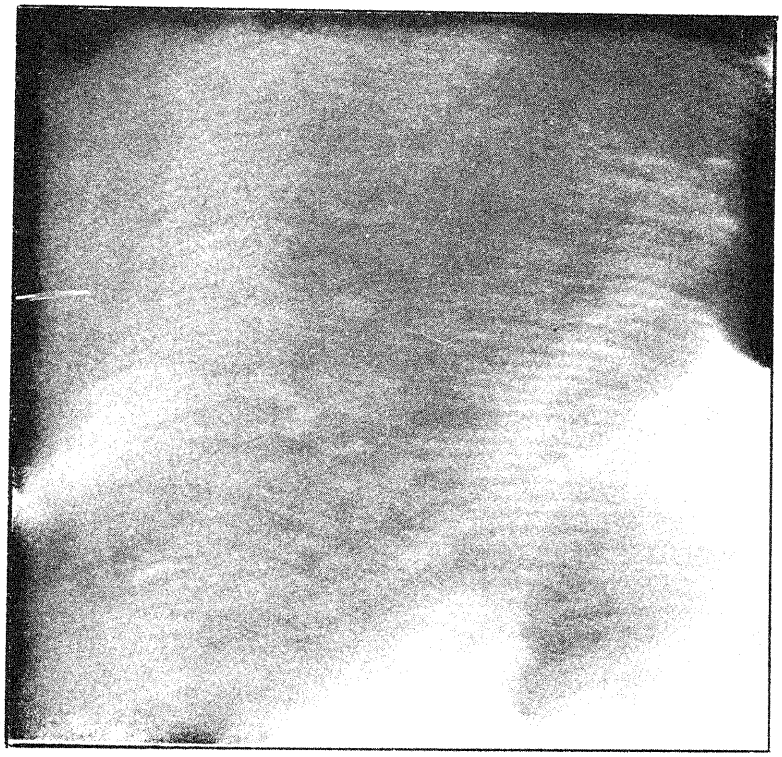

FIG. 9 RIPPLES-IN STAGE II CRACK. HIGH FREQUENCY FAILURE IN RR58 X14,000